



# Three-dimensional anthropometry in periorbital region

Yongwei Guo<sup>1,2^</sup>, Alexander C. Rokohl<sup>2^</sup>, Ming Lin<sup>3^</sup>, Ludwig M. Heindl<sup>2,4^</sup>

<sup>1</sup>Eye Center, Second Affiliated Hospital, School of Medicine, Zhejiang University, Hangzhou, China; <sup>2</sup>Department of Ophthalmology, University of Cologne, Faculty of Medicine and University Hospital Cologne, Cologne, Germany; <sup>3</sup>Department of Ophthalmology, Ninth People's Hospital, Shanghai Jiao Tong University School of Medicine, Shanghai, China; <sup>4</sup>Center for Integrated Oncology (CIO) Aachen-Bonn-Cologne-Duesseldorf, Cologne, Germany

**Contributions:** (I) Conception and design: LM Heindl, Y Guo; (II) Administrative support: LM Heindl; (III) Provision of study materials or patients: LM Heindl, AC Rokohl, Y Guo; (IV) Collection and assembly of data: AC Rokohl, Y Guo, M Lin; (V) Data analysis and interpretation: LM Heindl, M Lin, Y Guo; (VI) Manuscript writing: All authors; (VII) Final approval of manuscript: All authors.

**Correspondence to:** Ludwig M. Heindl, MD. Department of Ophthalmology, University of Cologne, Faculty of Medicine and University Hospital Cologne, Kerpener Strasse 62, 50937 Cologne, Germany. Email: ludwig.heindl@uk-koeln.de; Yongwei Guo, MD. Eye Center, Second Affiliated Hospital, School of Medicine, Zhejiang University, 88 Jiefang Road, Hangzhou 310009, China. Email: 10211220058@fudan.edu.cn.

**Abstract:** Anthropometry can analyze the size, weight, and proportion of the human body objectively and quantitatively to supplement the visual assessment. Various non-invasive three-dimensional (3D) anthropometric techniques have been applied to assess soft tissues' 3D morphology in the clinical practice. Among them, non-invasive stereophotogrammetry and laser scanning techniques are becoming increasingly popular in craniofacial surgery and plastic surgery. They have been applied for craniofacial growth estimation and morphometric investigation, genetic and acquired malformation diagnosis, as well as orthodontic or surgical treatment arrangement and outcome evaluation. However, few studies have been published for assessing the 3D morphology of soft tissues in the periorbital region. This paper reviews the studies involving the application and evaluation of the increasingly popular 3D photogrammetry in the periorbital region. These studies proposed detailed and standardized protocols for three-dimensionally assessing linear, curvilinear, angular, as well as volumetric measurements, and verified its high reliability in the periorbital region (even higher than caliper-derived direct measurements). In the future, reliable and accurate 3D imaging techniques, as well as standardized analyzing protocols, may find applications in following up morphological growth, preoperatively diagnosing and assessing patient periorbital conditions, planning surgical procedures, postoperatively evaluating treatment outcomes of a specific procedure, and comparing the differences in surgical results between various procedures, studies, as well as populations.

**Keywords:** Three-dimensional (3D); photogrammetry; periorbital soft tissue; eye; face

Received: 16 May 2020; Accepted: 12 November 2020; Published: 15 March 2021.

doi: 10.21037/aes-20-99

**View this article at:** <http://dx.doi.org/10.21037/aes-20-99>

Anthropometry can analyze the size, weight, and proportion of the human body objectively and quantitatively to supplement the visual assessment (1). Many scientific fields have employed anthropometric data for various aims, especially in craniofacial surgery, breast plastic surgery, and

oculoplastic and reconstructive surgery (2-4). Anthropometry of the craniofacial soft tissue plays an essential role in the clinical practice by measuring various parameters between landmarks defined on the head, face, and ears. It can be applied for craniofacial growth estimation and morphometric

<sup>^</sup> ORCID: Yongwei Guo: 0000-0001-9195-0770; Alexander C. Rokohl: 0000-0002-0224-3597; Ming Lin: 0000-0001-6467-4643; Ludwig M. Heindl: 0000-0002-4413-6132.

investigation, genetic and acquired malformation diagnosis, as well as orthodontic or surgical treatment arrangement and outcome evaluation (5-7).

However, few studies have been published for assessing the 3D morphology of soft tissues in the periorbital region. Therefore, this paper aims to review the application and evaluation of the increasingly popular three-dimensional (3D) photogrammetry in the periorbital region. In this study, a PubMed database search was performed to identify relevant publications using the search algorithm [(photogrammetry) AND (three-dimension\*)] AND [(eye) OR (face)]. We also screened relevant research missed in this search algorithm from the reference lists of specific full-text papers. After looking through these papers, we summarized the landmarks when measuring the periorbital region three-dimensionally and included the typical studies.

### **Traditional anthropometry for the craniofacial region**

Traditionally, craniofacial anthropometry is mainly obtained by direct anthropometry and two-dimensional (2D) photogrammetry or cephalometry. However, people are increasingly aware of their disadvantages. These technologies cannot completely capture and quantify the complex 3D craniofacial morphology of the human (8). Besides, the direct technique demands massive measuring time, close physical contact, and excellent patient compliance; 2D photogrammetry lacks proper 3D morphological depth (9); cephalometry exposes the subjects to hazardous ionizing radiation.

### **3D anthropometry for the craniofacial region**

To date, various non-invasive 3D capture and quantification techniques have been applied in the clinic practice, e.g., magnetic resonance imaging, quantitative ultrasound, laser scan, and stereophotogrammetry. Knoops *et al.* (10) compared the properties of four 3D scanning systems, including the 1.5T clinical MR Avanto Scanner, the static 3dMDface System, the handheld M4D Scan, and the Structure Sensor. They concluded that the 3dMDface System and M4D Scan supply high-quality results; the scanner choice is up to clinical and technical requirements; compact, handheld 3D systems would become increasingly popular in the near future.

Compared with traditional 3D techniques, laser scanning and stereophotogrammetry are highly accurate and precise,

rapid and straightforward, and non-invasive. Besides, they can quantify various parameters, including linear distances, curvatures, angles, volumes (11), and surface areas (10). In contrast to laser scanning technique, stereophotogrammetry captures high-resolution 3D surface images at a quicker speed, which is especially beneficial for young children and patients with insufficient compliance. Previous studies have been applied to assess morphological alterations with aging (12,13), record characteristics of healthy subjects, and evaluate the conditions of impairment or malformation such as the cleft palate (14-17).

### **3D photogrammetry for the periorbital region**

Thus far, a series of research mainly studied the 3D photogrammetry concerning the maxillofacial morphology. In contrast, few studies have focused on the 3D evaluation of the surface in the periorbital region. Gibelli *et al.* (18) captured face images of 14 volunteers using both stereophotogrammetry and a laser scanner. They then verified the concordance between 14 linear distances, 12 angles, as well as facial area and volume. They located the periorbital landmark of lateral canthus and measured the palpebral fissure's inclination versus the horizontal plane. Gibelli *et al.* (14) conducted another research to validate a portable stereophotogrammetric device versus a static one to verify its applicability to 3D facial analysis. They acquired 3D facial photographs of 40 volunteers using portable and static devices. The medial canthus and lateral canthus were set as periorbital landmarks.

Regarding research focusing on the periorbital region, Li *et al.* (19) performed a cross-sectional study using a standardized 2D photogrammetry obtained from 162 Chinese young adults aged 20 to 30. They defined several landmarks, including palpebral superius and palpebral inferius (the highest and lowest points of the free margin of upper eyelid), medial canthus and lateral canthus (the soft tissue point at the inner and outer commissure of the palpebral fissure), as well as upper lid crease superius (the highest point of double lid crease). Subsequently, a series of linear and angular anthropometric parameters between these landmarks were measured, i.e., palpebral fissure length and height, inter- and outer-canthal width, crease height, angles of the medial canthus and lateral canthus, as well as the axis of the palpebral fissure. They then calculated the palpebral fissure index, canthal index, and angular index. Jayaratne *et al.* (20) conducted the first study creating a database of 3D periorbital anthropometric norms applying

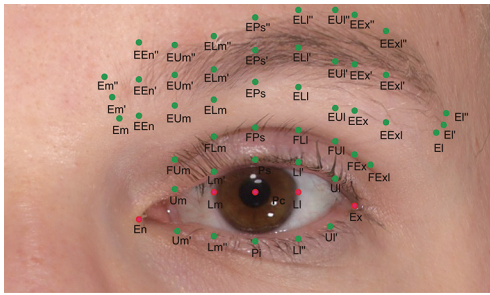


**Figure 1** Fifty-two 3D anthropometric landmarks of the periocular region elucidated in a 2D modality. Five prime points are located on 3D surface models, including the medial canthus, lateral canthus, pupillary center, as well as the medial and lateral limbus (horizontal to the pupillary center). Then, most of the other digital landmarks were identified vertically to the points mentioned above. Adapted by permission from Springer Nature from reference (23). 3D, three-dimensional; 2D, two-dimensional.

3D stereophotogrammetry. They adopted a 3dMDFace system to acquire the craniofacial images of 103 Chinese subjects aged between 18 and 35. They then measured linear distances (intercanthal width, binocular width, eye fissure height, and eye fissure length) between several anthropometric landmarks (palpebrale superius, palpebrale inferius, lateral canthus, and medial canthus) identified on these digital 3D images. Jodeh *et al.* (21) proposed a new method to measure normative facial projection relative to the pupil. They adopted the landmarks of bilateral pupils, supra- and infra-orbital rims, lateral orbital rims, lateral and medial canthi, as well as midline nasal radix.

However, no research in 3D periorbital anthropometry has been performed in surgery planning and treatment outcome evaluation. That is partially due to the lack of detailed and standardized 3D periorbital landmarks as well as normative anthropometric parameters database in the periorbital region regarding linear distance, angle, curvature, among others. With standardized parameters, surgeons may compare different results in various studies and precisely follow up the pre- and postoperative 3D morphological alterations of the surface in the periorbital region.

#### ***Standardized 3D anthropometric landmark localization protocol for the periorbital region***

Guo *et al.* (22,23) proposed a novel standardized 3D anthropometric landmarks localization protocol for the

periocular (or periorbital) region, which is beneficial for standardizing 3D periorbital anthropometry and minimizing the localization errors among various studies. The subjects were seated in front of a 3D camera. They opened their eyes and gazed forward into a mirror in the middle of the 3D camera. After taking a 3D photograph of each subject, an experienced researcher performed this protocol with the aid of coordinate axes in software. At the beginning of this protocol, five landmarks were set as prime points on each 3D periorbital model. They are the pupillary center (Pc), the intersection point of the medial or lateral limbus and the horizontal line passing through the pupillary center (Lm or Ll), medial canthus (En), and lateral canthus (Ex). The En was identified as the vertex of the inner canthal angle, and the Ex was localized at the lateral commissure of the superior and inferior eyelash lines. These five landmarks were proved to be simple, reliable, and easily identifiable. Subsequently, a series of landmarks were placed vertically to one of these five landmarks (*Figure 1* and *Table 1*).

Furthermore, they defined the periorbital parameters between these landmarks as three categories, i.e., palpebral fissure-related, upper lid fold-related, and brow-related parameters (*Table 2*) (22,23). Besides, they established a 3D periorbital morphology database for young Caucasians and analyzed the differences between sexes. They found a statistically significant difference in 63% of the linear distances, curvatures, angles, and indices between sexes. A correlation between aesthetic assessment and several periorbital parameters was also shown in this study (22). Specifically, a positive association with the aesthetic assessment was found in palpebral fissure height and eyebrow-palpebral margin distance (medial limbus); and a negative in canthal tilt, eyebrow-medial canthus distance, and eyebrow length.

In addition, attention has also been paid on the assessment of eyebrow height due to the close anatomic correlation between the eyebrow and the eyelid as well as the palpebral fissure. Various approaches have been proposed to describe the eyebrows' position across different ages, genders, and ethnicities (24-26). Guo *et al.* (22,23) measured the distances between the eyebrow (at inferior, middle, and superior margin points, respectively) and the upper palpebral margin (at landmarks corresponding to the above-mentioned prime points, i.e., the medial canthus, lateral canthus, pupillary center, medial limbus, and the lateral limbus). Kokubo *et al.* (27) adopted three landmarks, i.e., the medial canthus, the pupillary center, and the lateral canthus, to assess the eyebrow height on 2D photographs.

**Table 1** Definitions of 52 anthropometric periocular landmarks

Landmarks	Definition
En	Endocanthion (medial canthus), inner commissure of the palpebral fissure
Ex	Exocanthion (lateral canthus), outer commissure of the lower and upper eyelash roots of the palpebral fissure
Pc	Pupillary center
Lm	Medial corneoscleral limbus point horizontal to pupillary center
LI	Lateral corneoscleral limbus point horizontal to pupillary center
Em	Inferior margin point of the medial eyebrow end (sometimes locates at the same place with EEn); Em'', superior margin point; Em', middle point
EEn	Inferior margin point of eyebrow vertical to En; EEn'', superior margin point; EEn', middle point
Um	Middle point between En and Lm' at the upper palpebral margin on the lash roots
Um'	Middle point between En and Lm'' at the lower palpebral margin on the lash roots
FUm	Point vertical to Um at the lid fold superioris
EUm	Point vertical to Um at the inferior margin of eyebrows; EUm'', superior margin point; EUm', middle point
Lm'	Point vertical to Lm at the upper palpebral margin on the lash roots
Lm''	Point vertical to Lm at the lower palpebral margin on the lash roots
FLm	Point vertical to Lm at the lid fold superioris
ELm	Point vertical to Lm at the inferior margin of eyebrows; ELm'', superior margin point; ELm', middle point
Ps	Palpebrale superioris, point vertical to Pc at the upper palpebral margin on the lash roots
Pi	Palpebrale inferioris, point vertical to Pc at the lower palpebral margin on the lash roots
FPS	Point vertical to Pc at the lid fold superioris
EPS	Point vertical to Pc at the inferior margin of eyebrows; EPS'', superior margin point; EPS', middle point
LI'	Point vertical to LI at the upper palpebral margin on the lash roots
LI''	Point vertical to LI at the lower palpebral margin on the lash roots
FLI	Point vertical to LI at the lid fold superioris
ELI	Point vertical to LI at the inferior margin of eyebrows; ELI'', superior margin point; ELI', middle point
UI	The middle between Ex and LI' at the upper palpebral margin on the lash roots
UI'	The middle between Ex and LI'' at the lower palpebral margin on the lash roots
FUI	Point vertical to UI at the lid fold superioris
EUI	Point vertical to UI at the inferior margin of eyebrows; EUI'', superior margin point; EUI', middle point
FEx	Point vertical to Ex at the lid fold superioris
EEx	Point vertical to Ex at the inferior margin of eyebrows; EEx'', superior margin point; EEx', middle point
FExl	Point vertical to Ex at the lid fold superioris in lateral view
EExl	Point vertical to Ex at the inferior margin of eyebrows in lateral view; EExl'', superior margin point; EExl', middle point
EI	Inferior margin of the lateral eyebrow end; EI'', superior margin point; EI', middle point

Adapted by permission from Springer Nature from reference (23).

**Table 2** List of 49 periocular measurements

Definition	Abbreviation	Landmarks
Linear distances		
Palpebral fissure width	PFW	En-Ex
Palpebral fissure height	PFH	Ps-Pi
Eyebrow-endocanthion distance of the inferior, middle, or superior point	EEnD_I, EEnD_M, or EEnD_S	EEn-En
Upper lid fold-palpebral margin distance (medial)	FPDm	FUm-Um
Eyebrow-palpebral margin distance (medial) of the inferior, middle, or superior point	EPDm_I, EPDm_M, or EPDm_S	EUm-Um
Upper lid fold-palpebral margin distance (medial limbus)	FLmD	FLm-Lm'
Eyebrow-palpebral margin distance (medial limbus) of the inferior, middle, or superior point	ELmD_I, ELmD_M, or ELmD_S	ELm-Lm'
Upper lid fold-palpebral margin distance, similar to upper lid fold height	FPD	Ps-FPs
Eyebrow-palpebral margin (Ps) distance of the inferior (similar to upper lid height), middle, or superior point	EPD_I, EPD_M, or EPD_S	Ps-EPs
Upper lid fold-palpebral margin distance (lateral limbus)	FLID	FLI-LI'
Eyebrow-palpebral margin distance (lateral limbus) of the inferior, middle, or superior point	ELID_I, ELID_M, or ELID_S	ELI-LI'
Upper lid fold-palpebral margin distance (lateral)	FPDI	FUI-UI
Eyebrow-palpebral margin distance (lateral) of the inferior, middle, or superior point	EPDI_I, EPDI_M, or EPDI_S	EUI-UI
Upper lid fold-exocanthion distance	FExD	FEx-Ex
Eyebrow-exocanthion distance of the inferior, middle, or superior point	EExD_I, EExD_M, or EExD_S	EEx-Ex
Upper lid fold-exocanthion distance (lateral)	FExDI	FExI-Ex
Eyebrow-exocanthion distance (lateral) of the inferior, middle, or superior point	EExDI_I, EExDI_M, or EExDI_S	EExI-Ex
Iris diameter	ID	Lm-LI
Inner intercanthal distance	EnD	En (left)-En (right)
Interpupillary distance	PD	Pc (left)-Pc (right)
Outer intercanthal distance	ExD	Ex (left)-Ex (right)
Curvatures		
Upper palpebral margin length	UPML	En-Um-Lm'-Ps-LI'-UI-Ex
Upper palpebral margin length (more points)	UPMLm	Including 4 more midpoints between Lm'-Ps-LI'-UI-Ex
Lower palpebral margin length	LPML	En-Um'-Lm''-Pi-LI''-UI'-Ex
Lower palpebral margin length (more points)	LPMLm	Including 4 more midpoints between Lm''-Pi-LI''-UI'-Ex
Inferior eyebrow length	EL_I	Em-EEn-EUm-ELm-EPs-ELI-EUI-EEx-EEEx-EI
Middle eyebrow length	EL_M	Em'-EEn'-EUm'-ELm'-EPs'-ELI'-EUI'-EEx'-EEEx'-EI'
Superior eyebrow length	EL_S	Em''-EEn''-EUm''-ELm''-EPs''-ELI''-EUI''-EEx''-EEEx''-EI''

**Table 2** (continued)

Table 2 (continued)

Definition	Abbreviation	Landmarks
Angles		
Medial canthal angle	MCA	Ps-En-Pi
Medial canthal angle (medial)	MCAm	Um-En-Um'
Lateral canthal angle	LCA	Ps-Ex-Pi
Lateral canthal angle (medial)	LCAm	Ul-Ex-Ul'
Canthal tilt	CT	Ex (left)-En (left)-En (right), or Ex (right)-En (right)-En (left)

Adapted by permission from Springer Nature from reference (23).

They drew a horizontal plane between the right and left medial canthi. The pupillary center and lateral canthus were reflected on this plane. Eyebrow height was deemed the distance between these points on the plane and the eyebrow's superior margin. Besides, other studies involved the distance between the pupillary center and the lower eyebrow margin (28), the distance between the pupillary light reflex and the midpoint of the eyebrow (29), among others.

### Evaluation of 3D photogrammetry for the periorbital region

Before extensively spreading in clinical practice, all technologies should be validated entirely for measurement errors (30). Ulijaszek *et al.* (31) reviewed various anthropometric measurement error types and critically evaluated the methods of estimating measurement error. Although various terms have been reported to evaluate anthropometric measurement error in previous studies, two categories of possible measurement error are predominantly described as following: (I) the degree to which repeated measures obtain the same value; and (II) the close degree for a measurement to its "true" value.

#### Reliability

Of the first category, reliability, unreliability, precision, imprecision, and reproducibility are the most commonly used terminology in addition to undependability. The studies that evaluated the reliability of 3D photogrammetry commonly meant to figure out the degree of unreliability. Precision and imprecision have been the most commonly used evaluation index for anthropometric measurement errors (14,18,23,32-39). Imprecision is the variance of

repeated measurements, e.g., intra-observer measurement error (i.e., within-observer error) and inter-observer measurement error (i.e., between-observer error). Ulijaszek *et al.* (31) described the calculating procedures of technical error of measurement (TEM), relative TEM (rTEM), coefficient of reliability (R), and intraclass correlation coefficient (ICC) in detail to estimate imprecision. Guo *et al.* (23,39) evaluated the intra- and inter-observer reliability as well as intra-method reliability of their standardized periorbital 3D photogrammetry technique. They calculated TEM, rTEM, total TEM, mean absolute difference (MAD), relative error measurement (REM), and ICC. The calculation procedure and acceptable levels of measurement error have been proposed as follows:

- (I) The ICC ranges from 0 to 1, which indicates the reliability from low to high levels. Less than 0.4 is defined as poor consistency, 0.4 to 0.75 satisfactory consistency, and equal or more than 0.75 excellent consistency (31).
- (II) The MAD is calculated by averaging the absolute differences between the two sets of measurements.
- (III) The TEM is expressed as the measurement error variance's square root. Two units (millimeter or degree) has been deemed acceptable in previous 3D craniofacial photogrammetry studies for MAD and TEM (34).
- (IV) REM and rTEM represent the measurement error relative to the measurements' size. They are calculated by dividing the MAD or TEM of a specific variable by the mean of the two repeated measurements and then multiplying the outcome by 100%. They are recommended to compare the imprecision of different parameters or parameters in various population groups or studies. Less than 1% is deemed excellent consistency, between 1%

and 3.9% very good consistency, between 4% and 6.9% good consistency, between 7% and 9.9% moderate consistency, equal or more than 10% poor consistency (32,40).

- (V) Total TEM is acquired by summing the square of all TEM and then taking the square root. The relative total TEM (rTotal TEM) is calculated and expressed as percent similar to rTEM. Both total TEM and rTotal TEM are used to distinguish the measurement errors across studies involving more than one observer and calculating both intra- and inter-observer TEM (31).

Andrade *et al.* (40) analyzed the repeatability of a stereophotogrammetry system for evaluating facial morphology. They marked 11 maxillofacial reference landmarks on each subject's face, including the glabella, nasion, pronasale, columella, subnasale, labiale superius, labiale inferius, labiale sublabiale, pogonium, menton, tragus. Nine angular measurements and two linear measurements were obtained. They calculated the MAD, REM, TEM, ICC, and conducted a Bland-Altman analysis for repeatability analysis. They found that the nasolabial and mentolabial angles were larger than 2° (clinical limit) in TEM. All measurements were between good and excellent consistency for REM, except for the maxillofacial angle (moderate). The nasolabial, mentolabial, facial convexity, full facial convexity, maxillofacial, and nasofrontal angles were deemed excellent for ICC. In the end, they concluded that the stereophotogrammetry was repeatable and may give accurate measures within their references.

As for the periorbital region, Jodeh *et al.* (21) found less than 0.5 mm of standard deviations for repeat measures of bilateral pupils' landmarks, supra- and infra-orbital rims, lateral orbital rims, lateral and medial canthi, as well as midline nasal radix. Intra-rater reliability was high for all these landmarks (ICC: 0.93 to 0.99). Inter-rater reliability was excellent for all landmarks except for the lateral canthion. They concluded that their technique might apply to evaluate surgery outcomes and growth alterations on the facial project. Guo *et al.* (23) identified 52 periorbital landmarks and then analyzed the intra-rater, inter-rater, and intra-method reliability of 49 linear, curvilinear, as well as angular measurements. For intra-rater 1 and intra-rater 2 reliability, they found highly reliable results for MAD (0.59 and 0.68 unit), REM (2.66% and 3.08%), TEM (0.59 and 0.66 unit), rTEM (2.71% and 2.96%), and ICC (0.98). For inter-rater reliability, the results showed 0.94 unit in MAD, 4.06% in REM, 0.89 unit in TEM,

3.94% in rTEM, and 0.97 in ICC. Regarding intra-method reliability, the MAD was 0.98 unit, REM 4.66%, TEM 0.96 unit, rTEM 4.64%, and ICC 0.96. They concluded that this stereophotogrammetry and the landmark localization procedure were highly reliable for periorbital anthropometry.

Besides, they also evaluated the reliability of 22 periorbital measurements obtained by direct anthropometry, 2D photogrammetry, or 3D stereophotogrammetry (39). They then compared the reliability levels of each measurement among these three techniques. The results showed that, for direct, 2D, and 3D techniques, overall intra-rater ICC was 0.88, 0.99, and 0.98, respectively; overall intra-rater MAD was 0.84 mm, 0.26 units, and 0.35 units, respectively; overall intra-rater TEM was 0.85 mm, 0.25, and 0.32 units, respectively; overall intra-rater REM was 6.46%, 1.69%, and 1.67%, respectively; overall intra-rater rTEM was 6.25%, 1.62%, and 2.12%, respectively. Furthermore, for 2D and 3D techniques, overall inter-rater ICC was 0.97 and 0.92; overall inter-rater MAD was 0.36 unit and 0.67 unit; overall inter-rater TEM was 0.36 unit and 0.65 unit; overall inter-rater REM was 2.74% and 5.11%; overall inter-rater rTEM was 2.78% and 5.12%. Therefore, they concluded that the stereophotogrammetry and their landmark identification protocol might be applied for 2D and 3D periorbital measurements due to the very good reliability.

### Accuracy

Of the second category, bias, validity, accuracy, and inaccuracy are the terms commonly used. Accuracy is the degree to which the "true" value of a measurement is given. Validity involved the value measured, which is conceptually approximate to accuracy. The measurement obtained by a gold standard tool is considered the "true" value of a characteristic in practice. Inaccuracy is a systematic bias that may occur due to the error from either equipment or measurement technique.

It is thought that complex equipment may yield a more significant inaccuracy of measurement than a simple one. Therefore, Ulijaszek and Kerr (31) believed that a simple tape measure is likely to give more accurate results than a sophisticated instrument involving sliding scales, e.g., anthropometers and stadiometers, while assessing the status of nutrition by measuring skinfolds. The calipers may compress the skin, causing surface deformation and landmarks displacement with corresponding soft tissue measurement differences.

Although direct anthropometry using sliding and spreading calipers may be inaccurate, it remains the gold standard for anthropometry in craniomaxillofacial surgery due to its simple, operable, and affordable characteristics. Therefore, various novel anthropometry techniques are commonly compared with the direct technique to evaluate their accuracy. Dindaroğlu *et al.* (34) compared 3D stereophotogrammetry with the direct and 2D photogrammetry techniques to evaluate 3D stereophotogrammetry accuracy in six profiles and four frontal parameters. They also examined the reliability coefficient between methods. Their results showed the highest MAD of 0.30 mm between direct and 2D techniques, 0.21 mm between direct and 3D techniques, and 0.5 mm between 2D and 3D techniques. As for reliability, the nasal tip protrusion was found the lowest agreement ICC value of 0.965 between 2D and 3D techniques. Weinberg (41) compared a set of 24 standard soft-tissue craniofacial linear distances between two datasets, i.e., the 3D facial norms obtained by stereophotogrammetry (n=2,454) and the Farkas craniofacial norms gained by direct anthropometry (n=2,326). To evaluate both data sets' discrepancy, they calculated standardized effect sizes (Cohen d) for all measurements to assess its overall direction and magnitude. The mean d value is positively correlated with the discrepancy across datasets, e.g., the higher the mean d value is, the greater is the discrepancy. They found a more significant discrepancy in measurements involving the landmarks of tragon (the point anterior to the external auditory canal at the upper margin of the tragus) and nasion (the intersection of the midline and the frontonasal suture). Besides, the width of nasolabial structures, the lip involving vermilion, and the palpebral fissure length was also found more considerable differences between the two datasets. Therefore, they concluded that there were considerable discrepancies between both norms obtained by 3D stereophotogrammetry or direct anthropometry.

Furthermore, previously validated stationary 3D surface imaging systems have been applied to validate recently invented low-cost and portable 3D imaging systems due to high accuracy and reliability. Camison *et al.* (32) took 3D facial photographs of 26 adult individuals with the handheld Vectra H1 and a previously validated 3D imaging system 3dMDface system. They then evaluated the error magnitude statistics of 136 linear facial distances and global root mean square (RMS) error of 26 surface -to surface comparisons. The results showed highly comparable measurements in these distances across both cameras (mean TEM =0.84 mm,

ranging between 0.19 and 1.54 mm). The mean RMS was 0.43 mm (ranging between 0.33 and 0.59 mm). Therefore, they concluded that 3D facial surface photographs captured with the portable system were adequately accurate for most clinical applications.

Besides, it is a challenge to perform direct anthropometry in the periorbital region. Involuntary blinking and soft tissue deformation increase the measurement errors, which is especially crucial for a small size. Furthermore, physical contact may injure the eyes' delicate structures, increase the operating time, and depend more on patient cooperation. Therefore, 3D anthropometry may be a future trend and become the gold standard for periorbital anthropometry in the future. In Weinberg's study (41), the author evaluated three periorbital parameters, i.e., inner canthal width, outer canthal width, and palpebral fissure length. A more significant discrepancy between 3D and direct anthropometric datasets was shown in palpebral fissure length. They attributed the significant discrepancy to inadequate open and relaxation of the eyes due to direct anthropometry's physical contact nature. Hyer *et al.* (42) conducted a cross-sectional study to assess the accuracy and inter-observer reliability of 3D stereophotogrammetry for volumetric measurements in the periorbital region. They also proposed a protocol for acquiring volumetric data using 3D systems in this region. Exactly, they took 3D photographs of 58 adult subjects on two independent occasions and then performed 40 different measurements of volume for each side. Subsequently, they calculated the mean periorbital volume alterations between different methods, i.e., two registration methods (facial landmarks tool and surface area paint tool), open or closed eyes, separate or integrated upper and lower eyelids, lower eyelid with or without mid-face (tear trough and palpebromalar groove). A significant difference was indicated between different methods of measurement. The most accurate method showed the mean alteration in volume of  $0.11 \pm 0.13$  mL. The highest agreement between two independent observers was 0.63 for ICC. As a conclusion, they claimed that the 3D imaging system is accurate and suitable for assessing periorbital volumetric alteration in clinical practice, with good inter-observer repeatability.

## Conclusions

In summary, 3D anthropometry has become increasingly popular in clinical practice to date. The current studies have proposed detailed and standardized protocols for three-



dimensionally assessing linear, curvilinear, angular, as well as volumetric measurements, and verified its high reliability in the periorbital region (even higher than caliper-derived direct measurements) (22,23,39,42). In the future, reliable and accurate 3D imaging techniques, as well as standardized analyzing protocols, may find applications in following up morphological growth, preoperatively diagnosing and assessing patient periorbital conditions, planning surgical procedures, postoperatively evaluating treatment outcomes of a specific procedure, and comparing the differences in surgical results between various procedures, studies, as well as populations.

### Acknowledgments

*Funding:* This study was supported by the Koeln Fortune Program/Faculty of Medicine, University of Cologne, Germany (No. 2680148101) and the State Scholarship Fund from China Scholarship Council, China (No. 201708080141).

### Footnote

*Provenance and Peer Review:* This article was commissioned by the editorial office, *Annals of Eye Science* for the series “Eyelid Surgery”. The article has undergone external peer review.

*Peer Review File:* Available at <http://dx.doi.org/10.21037/aes-20-99>

*Conflicts of Interest:* All authors have completed the ICMJE uniform disclosure form (available at <http://dx.doi.org/10.21037/aes-20-99>). The series “Eyelid Surgery” was commissioned by the editorial office without any funding or sponsorship. ML and LMH served as the unpaid Guest Editors of the series. LMH serves as an unpaid editorial board member of *Annals of Eye Science* from Dec 2019 to Nov 2021. The authors have no other conflicts of interest to declare.

*Ethical Statement:* The authors are accountable for all aspects of the work in ensuring that questions related to the accuracy or integrity of any part of the work are appropriately investigated and resolved.

*Open Access Statement:* This is an Open Access article distributed in accordance with the Creative Commons

Attribution-NonCommercial-NoDerivs 4.0 International License (CC BY-NC-ND 4.0), which permits the non-commercial replication and distribution of the article with the strict proviso that no changes or edits are made and the original work is properly cited (including links to both the formal publication through the relevant DOI and the license). See: <https://creativecommons.org/licenses/by-nc-nd/4.0/>.

### References

1. Aldridge K, Boyadjiev SA, Capone GT, et al. Precision and error of three-dimensional phenotypic measures acquired from 3dMD photogrammetric images. *Am J Med Genet A* 2005;138A:247-53.
2. Overschmidt B, Qureshi AA, Parikh RP, et al. A prospective evaluation of three-dimensional image simulation: patient-reported outcomes and mammometrics in primary breast augmentation. *Plast Reconstr Surg* 2018;142:133e-44e.
3. Suszynski TM, Serra JM, Weissler JM, et al. Three-dimensional printing in rhinoplasty. *Plast Reconstr Surg* 2018;141:1383-5.
4. Talbert L, Kau CH, Christou T, et al. A 3D analysis of Caucasian and African American facial morphologies in a US population. *J Orthod* 2014;41:19-29.
5. Tremp M, di Summa PG, Schaakxs D, et al. Nipple reconstruction after autologous or expander breast reconstruction: a multimodal and 3-dimensional analysis. *Aesthet Surg J* 2017;37:179-87.
6. Baik HS, Jeon JM, Lee HJ. Facial soft-tissue analysis of Korean adults with normal occlusion using a 3-dimensional laser scanner. *Am J Orthod Dentofacial Orthop* 2007;131:759-66.
7. Kau CH, Hunter LM, Hingston EJ. A different look: 3-dimensional facial imaging of a child with Binder syndrome. *Am J Orthod Dentofacial Orthop* 2007;132:704-9.
8. Nord F, Ferjencik R, Seifert B, et al. The 3dMD photogrammetric photo system in cranio-maxillofacial surgery: validation of interexaminer variations and perceptions. *J Craniomaxillofac Surg* 2015;43:1798-803.
9. Weinberg SM, Scott NM, Neiswanger K, et al. Digital three-dimensional photogrammetry: evaluation of anthropometric precision and accuracy using a Genex 3D camera system. *Cleft Palate Craniofac J* 2004;41:507-18.
10. Knoop PGM, Beaumont CAA, Borghi A, et al. Comparison of three-dimensional scanner systems for craniomaxillofacial imaging. *J Plast Reconstr Aesthet Surg*

- 2017;70:441-9.
11. Ramesh S, Johnson P, Sarcu D, et al. Gravity in midfacial aging: a 3-dimensional study. *Aesthet Surg J* 2021;41:143-51.
  12. Koudelová J, Brůžek J, Cagaňová V, et al. Development of facial sexual dimorphism in children aged between 12 and 15 years: a three-dimensional longitudinal study. *Orthod Craniofac Res* 2015;18:175-84.
  13. Lambros V. Facial aging: a 54-year, three-dimensional population study. *Plast Reconstr Surg* 2020;145:921-8.
  14. Gibelli D, Pucciarelli V, Cappella A, et al. Are portable stereophotogrammetric devices reliable in facial imaging? A validation study of VECTRA H1 device. *J Oral Maxillofac Surg* 2018;76:1772-84.
  15. Pucciarelli V, Bertoli S, Codari M, et al. Facial evaluation in holoprosencephaly. *J Craniofac Surg* 2017;28:e22-8.
  16. Pucciarelli V, Bertoli S, Codari M, et al. The face of Glut1-DS patients: a 3D craniofacial morphometric analysis. *Clin Anat* 2017;30:644-52.
  17. Gibelli D, De Angelis D, Poppa P, et al. An assessment of how facial mimicry can change facial morphology: implications for identification. *J Forensic Sci* 2017;62:405-10.
  18. Gibelli D, Pucciarelli V, Poppa P, et al. Three-dimensional facial anatomy evaluation: Reliability of laser scanner consecutive scans procedure in comparison with stereophotogrammetry. *J Craniomaxillofac Surg* 2018;46:1807-13.
  19. Li Q, Zhang X, Li K, et al. Normative anthropometric analysis and aesthetic indication of the ocular region for young Chinese adults. *Graefes Arch Clin Exp Ophthalmol* 2016;254:189-97.
  20. Jayaratne YS, Deutsch CK, Zwahlen RA. Normative findings for periocular anthropometric measurements among Chinese young adults in Hong Kong. *Biomed Res Int* 2013;2013:821428.
  21. Jodeh DS, Curtis H, Cray JJ, et al. Anthropometric evaluation of periorbital region and facial projection using three-dimensional photogrammetry. *J Craniofac Surg* 2018;29:2017-20.
  22. Guo Y, Schaub F, Mor JM, et al. A simple standardized three-dimensional anthropometry for the periocular region in a European Population. *Plast Reconstr Surg* 2020;145:514e-23e.
  23. Guo Y, Rokohl AC, Schaub F, et al. Reliability of periocular anthropometry using three-dimensional digital stereophotogrammetry. *Graefes Arch Clin Exp Ophthalmol* 2019;257:2517-31.
  24. Kunjur J, Sabesan T, Ilankovan V. Anthropometric analysis of eyebrows and eyelids: an inter-racial study. *Br J Oral Maxillofac Surg* 2006;44:89-93.
  25. Alex JC. Aesthetic considerations in the elevation of the eyebrow. *Facial Plast Surg* 2004;20:193-8.
  26. Price KM, Gupta PK, Woodward JA, et al. Eyebrow and eyelid dimensions: an anthropometric analysis of African Americans and Caucasians. *Plast Reconstr Surg* 2009;124:615-23.
  27. Kokubo K, Katori N, Hayashi K, et al. Evaluation of the eyebrow position after levator resection. *J Plast Reconstr Aesthet Surg* 2017;70:85-90.
  28. Rootman DB, Karlin J, Moore G, et al. The effect of ptosis surgery on brow position and the utility of preoperative phenylephrine testing. *Ophthal Plast Reconstr Surg* 2016;32:195-8.
  29. Nakra T, Modjtahedi S, Vrcek I, et al. The effect of upper eyelid blepharoplasty on eyelid and brow position. *Orbit* 2016;35:324-7.
  30. Schaaf H, Pons-Kuehnemann J, Malik CY, et al. Accuracy of three-dimensional photogrammetric images in non-synostotic cranial deformities. *Neuropediatrics* 2010;41:24-9.
  31. Ulijaszek SJ, Kerr DA. Anthropometric measurement error and the assessment of nutritional status. *Br J Nutr* 1999;82:165-77.
  32. Camison L, Bykowski M, Lee WW, et al. Validation of the Vectra H1 portable three-dimensional photogrammetry system for facial imaging. *Int J Oral Maxillofac Surg* 2018;47:403-10.
  33. Verhulst AC, Wesselius TS, Glas HH, et al. Accuracy and reproducibility of a newly developed tool for volume measurements of the arm using 3D stereophotogrammetry. *J Plast Reconstr Aesthet Surg* 2017;70:1753-9.
  34. Dindaroğlu F, Kutlu P, Duran GS, et al. Accuracy and reliability of 3D stereophotogrammetry: a comparison to direct anthropometry and 2D photogrammetry. *Angle Orthod* 2016;86:487-94.
  35. Lübbers HT, Medinger L, Kruse A, et al. Precision and accuracy of the 3dMD photogrammetric system in craniomaxillofacial application. *J Craniofac Surg* 2010;21:763-7.
  36. de Menezes M, Rosati R, Ferrario VF, et al. Accuracy and reproducibility of a 3-dimensional stereophotogrammetric imaging system. *J Oral Maxillofac Surg* 2010;68:2129-35.
  37. Sawyer AR, See M, Nduka C. Assessment of the reproducibility of facial expressions with 3-D stereophotogrammetry. *Otolaryngol Head Neck Surg*

- 2009;140:76-81.
38. Plooiij JM, Swennen GR, Rangel FA, et al. Evaluation of reproducibility and reliability of 3D soft tissue analysis using 3D stereophotogrammetry. *Int J Oral Maxillofac Surg* 2009;38:267-73.
39. Guo Y, Hou X, Rokohl AC, et al. Reliability of periocular anthropometry: a comparison of direct, 2-dimensional, and 3-dimensional techniques. *Dermatol Surg* 2020;46:e23-31.
40. Andrade LM, Rodrigues da Silva AMB, Magri LV, et al. Repeatability study of angular and linear measurements on facial morphology analysis by means of stereophotogrammetry. *J Craniofac Surg* 2017;28:1107-11.
41. Weinberg SM. 3D stereophotogrammetry versus traditional craniofacial anthropometry: Comparing measurements from the 3D facial norms database to Farkas's North American norms. *Am J Orthod Dentofacial Orthop* 2019;155:693-701.
42. Hyer JN, Murta F, Juniat VAR, et al. Validating three-dimensional imaging for volumetric assessment of periorbital soft tissue. *Orbit* 2021;40:9-17.

doi: 10.21037/aes-20-99

**Cite this article as:** Guo Y, Rokohl AC, Lin M, Heindl LM. Three-dimensional anthropometry in periorbital region. *Ann Eye Sci* 2021;6:8.